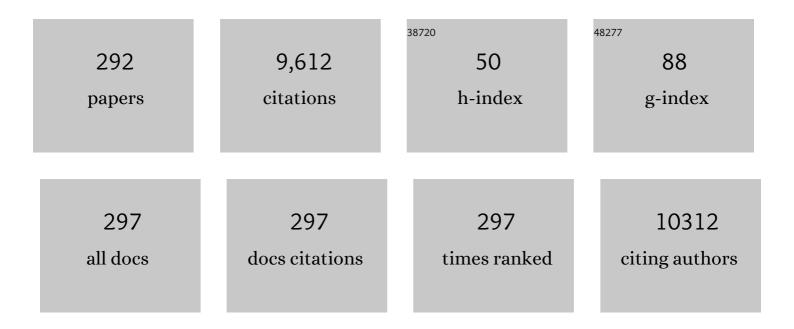
Qi Jie Wang

List of Publications by Year in descending order

Source: https://exaly.com/author-pdf/7138142/publications.pdf Version: 2024-02-01



OLLE WANC

#	Article	IF	CITATIONS
1	Broadband high photoresponse from pure monolayer graphene photodetector. Nature Communications, 2013, 4, 1811.	5.8	681
2	AtomicallyÂthin noble metal dichalcogenide: a broadband mid-infrared semiconductor. Nature Communications, 2018, 9, 1545.	5.8	367
3	Electrically pumped topological laser with valley edge modes. Nature, 2020, 578, 246-250.	13.7	341
4	Designer spoof surface plasmon structures collimate terahertz laser beams. Nature Materials, 2010, 9, 730-735.	13.3	260
5	A tunable 3D optofluidic waveguide dye laser via two centrifugal Dean flow streams. Lab on A Chip, 2011, 11, 3182.	3.1	246
6	Small-divergence semiconductor lasers by plasmonic collimation. Nature Photonics, 2008, 2, 564-570.	15.6	216
7	Allâ€Dielectric Active Terahertz Photonics Driven by Bound States in the Continuum. Advanced Materials, 2019, 31, e1901921.	11.1	210
8	Whispering-gallery mode resonators for highly unidirectional laser action. Proceedings of the National Academy of Sciences of the United States of America, 2010, 107, 22407-22412.	3.3	185
9	3 W continuous-wave room temperature single-facet emission from quantum cascade lasers based on nonresonant extraction design approach. Applied Physics Letters, 2009, 95, .	1.5	180
10	1.6W high wall plug efficiency, continuous-wave room temperature quantum cascade laser emitting at 4.6μm. Applied Physics Letters, 2008, 92, 111110.	1.5	171
11	Self-gating in semiconductor electrocatalysis. Nature Materials, 2019, 18, 1098-1104.	13.3	167
12	Lateral black phosphorene P–N junctions formed via chemical doping for high performance near-infrared photodetector. Nano Energy, 2016, 25, 34-41.	8.2	162
13	Integrated Terahertz Graphene Modulator with 100% Modulation Depth. ACS Photonics, 2015, 2, 1559-1566.	3.2	158
14	Engineering grain boundaries at theÂ2D limit for theÂhydrogen evolution reaction. Nature Communications, 2020, 11, 57.	5.8	153
15	Narrow bandgap oxide nanoparticles coupled with graphene for high performance mid-infrared photodetection. Nature Communications, 2018, 9, 4299.	5.8	151
16	Fast Photoresponse from 1T Tin Diselenide Atomic Layers. Advanced Functional Materials, 2016, 26, 137-145.	7.8	150
17	Tunable and switchable dual-wavelength Tm-doped mode-locked fiber laser by nonlinear polarization evolution. Optics Express, 2015, 23, 4369.	1.7	145
18	All-Optical Plasmonic Switches Based on Coupled Nano-disk Cavity Structures Containing Nonlinear Material. Plasmonics, 2011, 6, 753-759.	1.8	129

#	Article	IF	CITATIONS
19	High oscillator strength interlayer excitons in two-dimensional heterostructures for mid-infrared photodetection. Nature Nanotechnology, 2020, 15, 675-682.	15.6	129
20	Metal–Semiconductor Phaseâ€Transition in WSe _{2(1â€} <i>_x/i>₎Te₂<i>_x</i> Monolayer. Advanced Materials, 2017, 29, 1603991.</i>	11.1	123
21	Recent Progress in Short―to Longâ€Wave Infrared Photodetection Using 2D Materials and Heterostructures. Advanced Optical Materials, 2021, 9, 2001708.	3.6	118
22	Amplified Spontaneous Emission and Lasing from Lanthanide-Doped Up-Conversion Nanocrystals. ACS Nano, 2013, 7, 11420-11426.	7.3	116
23	Amorphizing noble metal chalcogenide catalysts at the single-layer limit towards hydrogen production. Nature Catalysis, 2022, 5, 212-221.	16.1	113
24	Broadly tunable one-way terahertz plasmonic waveguide based on nonreciprocal surface magneto plasmons. Optics Letters, 2012, 37, 1895.	1.7	112
25	High-Temperature Operation of Terahertz Quantum Cascade Laser Sources. IEEE Journal of Selected Topics in Quantum Electronics, 2009, 15, 952-967.	1.9	111
26	Temperature dependence of the electrical transport properties in few-layer graphene interconnects. Nanoscale Research Letters, 2013, 8, 335.	3.1	108
27	Directional emission and universal far-field behavior from semiconductor lasers with limaçon-shaped microcavity. Applied Physics Letters, 2009, 94, .	1.5	103
28	Graphene-based tunable plasmonic Bragg reflector with a broad bandwidth. Optics Letters, 2014, 39, 271.	1.7	98
29	High-power graphene mode-locked Tm/Ho co-doped fiber laser with evanescent field interaction. Scientific Reports, 2015, 5, 16624.	1.6	92
30	Suppressing spatiotemporal lasing instabilities with wave-chaotic microcavities. Science, 2018, 361, 1225-1231.	6.0	77
31	Nonlinear absorption of SWNT film and its effects to the operation state of pulsed fiber laser. Optics Express, 2014, 22, 17227.	1.7	76
32	Single-wall carbon nanotubes and graphene oxide-based saturable absorbers for low phase noise mode-locked fiber lasers. Scientific Reports, 2016, 6, 25266.	1.6	74
33	A high performance, visible to mid-infrared photodetector based on graphene nanoribbons passivated with HfO ₂ . Nanoscale, 2016, 8, 327-332.	2.8	74
34	Emerging High-Performance SnS/CdS Nanoflower Heterojunction for Ultrafast Photonics. ACS Applied Materials & Interfaces, 2020, 12, 43098-43105.	4.0	74
35	High performance quantum cascade lasers based on three-phonon-resonance design. Applied Physics Letters, 2009, 94, .	1.5	71
36	Photocurrent generation in lateral graphene p-n junction created by electron-beam irradiation. Scientific Reports, 2015, 5, 12014.	1.6	69

#	Article	IF	CITATIONS
37	Modelling of free-form conformal metasurfaces. Nature Communications, 2018, 9, 3494.	5.8	65
38	Semiconductor lasers with integrated plasmonic polarizers. Applied Physics Letters, 2009, 94, .	1.5	64
39	Massively parallel ultrafast random bit generation with a chip-scale laser. Science, 2021, 371, 948-952.	6.0	64
40	Limiting Factors to the Temperature Performance of THz Quantum Cascade Lasers Based on the Resonant-Phonon Depopulation Scheme. IEEE Transactions on Terahertz Science and Technology, 2012, 2, 83-92.	2.0	59
41	Ultra-confined surface phonon polaritons in molecular layers of van der Waals dielectrics. Nature Communications, 2018, 9, 1762.	5.8	59
42	High-power thulium fiber laser Q switched with single-layer graphene. Optics Letters, 2014, 39, 614.	1.7	58
43	Hybrid Graphene/Gold Plasmonic Fiberâ€Optic Biosensor. Advanced Materials Technologies, 2017, 2, 1600185.	3.0	58
44	Electrically Pumped Midâ€Infrared Random Lasers. Advanced Materials, 2013, 25, 6859-6863.	11.1	57
45	Tunable grapheneâ€based plasmonic waveguides: nano modulators and nano attenuators. Laser and Photonics Reviews, 2014, 8, 569-574.	4.4	57
46	Monolithic high-index contrast grating: a material independent high-reflectance VCSEL mirror. Optics Express, 2015, 23, 11674.	1.7	57
47	Beam engineering of quantum cascade lasers. Laser and Photonics Reviews, 2012, 6, 24-46.	4.4	56
48	Visible Range Plasmonic Modes on Topological Insulator Nanostructures. Advanced Optical Materials, 2017, 5, 1600768.	3.6	55
49	Quantum cascade lasers with integrated plasmonic antenna-array collimators. Optics Express, 2008, 16, 19447.	1.7	54
50	Photonic microwave phase shifter/modulator based on a nonlinear optical loop mirror incorporating a Mach-Zehnder interferometer. Optics Letters, 2007, 32, 745.	1.7	53
51	Surface magneto plasmons and their applications in the infrared frequencies. Nanophotonics, 2015, 4, 383-396.	2.9	51
52	Widely tunable Tm-doped mode-locked all-fiber laser. Scientific Reports, 2016, 6, 27245.	1.6	50
53	SnS ₂ Nanosheets for Er-Doped Fiber Lasers. ACS Applied Nano Materials, 2020, 3, 674-681.	2.4	49
54	All-fiber multiwavelength thulium-doped laser assisted by four-wave mixing in highly germania-doped fiber. Optics Express, 2015, 23, 340.	1.7	48

#	Article	IF	CITATIONS
55	High-Performance, Polarization-Sensitive, Long-Wave Infrared Photodetection <i>via</i> Photothermoelectric Effect with Asymmetric van der Waals Contacts. ACS Nano, 2022, 16, 295-305.	7.3	47
56	Numerical Study of Gain-Assisted Terahertz Hybrid Plasmonic Waveguide. Plasmonics, 2012, 7, 571-577.	1.8	46
57	All-normal-dispersion passively mode-locked Yb-doped fiber ring laser based on a graphene oxide saturable absorber. Laser Physics Letters, 2013, 10, 075108.	0.6	46
58	9  μm few-cycle optical parametric chirped-pulse amplifier based on LiGaS ₂ . Optics Letters 2019, 44, 2422.	^{5,} 1.7	43
59	Broadband Saturable Absorption of Graphene Oxide Thin Film and Its Application in Pulsed Fiber Lasers. IEEE Journal of Selected Topics in Quantum Electronics, 2014, 20, 441-447.	1.9	42
60	Tunable Subwavelength Terahertz Plasmonic Stub Waveguide Filters. IEEE Nanotechnology Magazine, 2013, 12, 1191-1197.	1.1	40
61	Room-temperature mid-infrared photodetector in all-carbon graphene nanoribbon-C_60 hybrid nanostructure. Optica, 2016, 3, 979.	4.8	40
62	Plasmonics for Laser Beam Shaping. IEEE Nanotechnology Magazine, 2010, 9, 11-29.	1.1	39
63	1867–2010 nm tunable femtosecond thulium-doped all-fiber laser. Optics Express, 2017, 25, 8997.	1.7	39
64	Resonant nanostructures for highly confined and ultra-sensitive surface phonon-polaritons. Nature Communications, 2020, 11, 1863.	5.8	39
65	Theoretical investigation of injection-locked high modulation bandwidth quantum cascade lasers. Optics Express, 2012, 20, 1450.	1.7	38
66	Switchable multi-wavelength Tm-doped mode-locked fiber laser. Optics Letters, 2015, 40, 1916.	1.7	37
67	All Inorganic Mixed Halide Perovskite Nanocrystal–Graphene Hybrid Photodetector: From Ultrahigh Gain to Photostability. ACS Applied Materials & Interfaces, 2019, 11, 27064-27072.	4.0	37
68	Slowing down terahertz waves with tunable group velocities in a broad frequency range by surface magneto plasmons. Optics Express, 2012, 20, 10071.	1.7	36
69	Multimicrojoule GaSe-based midinfrared optical parametric amplifier with an ultrabroad idler spectrum covering 42–16  μm. Optics Letters, 2019, 44, 1003.	1.7	35
70	Anomalous Single-Mode Lasing Induced by Nonlinearity and the Non-Hermitian Skin Effect. Physical Review Letters, 2022, 129, .	2.9	35
71	A Simple Nanometeric Plasmonic Narrow-Band Filter Structure Based on Metal–Insulator–Metal Waveguide. IEEE Nanotechnology Magazine, 2011, 10, 1371-1376.	1.1	34
72	Deformed microcavity quantum cascade lasers with directional emission. New Journal of Physics, 2009, 11, 125018.	1.2	33

#	Article	IF	CITATIONS
73	All-fiber short-wavelength tunable mode-locked fiber laser using normal dispersion thulium-doped fiber. Optics Express, 2020, 28, 17570.	1.7	33
74	Investigation of Multilayer Subwavelength Metallic-Dielectric Stratified Structures. IEEE Journal of Quantum Electronics, 2012, 48, 1554-1559.	1.0	32
75	High performance infrared photodetectors up to 28 µm wavelength based on lead selenide colloidal quantum dots. Optical Materials Express, 2017, 7, 2326.	1.6	32
76	GaAs/Al0.15Ga0.85As terahertz quantum cascade lasers with double-phonon resonant depopulation operating up to 172 K. Applied Physics Letters, 2010, 97, 131111.	1.5	31
77	Converting surface plasmon to spatial Airy beam by graded grating on metal surface. Optics Letters, 2013, 38, 1733.	1.7	31
78	Pseudo-magnetic field-induced slow carrier dynamics in periodically strained graphene. Nature Communications, 2021, 12, 5087.	5.8	31
79	Single-mode surface-emitting concentric-circular-grating terahertz quantum cascade lasers. Applied Physics Letters, 2013, 102, 031119.	1.5	29
80	Gain competition in dual wavelength quantum cascade lasers. Optics Express, 2010, 18, 9900.	1.7	28
81	Strong Plasmon–Exciton Interactions on Nanoantenna Array–Monolayer WS ₂ Hybrid System. Advanced Optical Materials, 2020, 8, 1901002.	3.6	28
82	Mid-infrared photonics and optoelectronics in 2D materials. Materials Today, 2021, 51, 294-316.	8.3	28
83	All-fiber Fourier filter flat-top interleaver design with specified performance parameters. Optical Engineering, 2003, 42, 3172.	0.5	27
84	Efficient structure for optical interleavers using superimposed chirped fiber Bragg gratings. IEEE Photonics Technology Letters, 2005, 17, 387-389.	1.3	27
85	A Nanoplasmonic High-Pass Wavelength Filter Based on a Metal-Insulator-Metal Circuitous Waveguide. IEEE Nanotechnology Magazine, 2011, 10, 1357-1361.	1.1	27
86	Designer Multimode Localized Random Lasing in Amorphous Lattices at Terahertz Frequencies. ACS Photonics, 2016, 3, 2453-2460.	3.2	27
87	Room-Temperature, Wide-Band, Quantum Well Infrared Photodetector for Microwave Optical Links at 4.9 μm Wavelength. ACS Photonics, 2018, 5, 3689-3694.	3.2	27
88	Radiation Enhancement by Graphene Oxide on Microelectromechanical System Emitters for Highly Selective Gas Sensing. ACS Sensors, 2019, 4, 2746-2753.	4.0	27
89	Surface-emitting terahertz quantum cascade laser source based on intracavity difference-frequency generation. Applied Physics Letters, 2008, 93, 161110.	1.5	26
90	High-power passively Q-switched thulium fiber laser with distributed stimulated Brillouin scattering. Optics Letters, 2013, 38, 5474.	1.7	26

#	Article	IF	CITATIONS
91	A metal–dielectric–graphene sandwich for surface enhanced Raman spectroscopy. Nanoscale, 2014, 6, 9925-9929.	2.8	26
92	High-Throughput Multiple Dies-to-Wafer Bonding Technology and III/V-on-Si Hybrid Lasers for Heterogeneous Integration of Optoelectronic Integrated Circuits. Frontiers in Materials, 2015, 2, .	1.2	26
93	Mid-IR supercontinuum pumped by femtosecond pulses from thulium doped all-fiber amplifier. Optics Express, 2016, 24, 13939.	1.7	26
94	Gigahertz surface acoustic wave generation on ZnO thin films deposited by radio frequency magnetron sputtering on III-V semiconductor substrates. Journal of Vacuum Science & Technology B, 2008, 26, 1848-1851.	1.3	25
95	Room temperature enhanced red emission from novel Eu ^{3 +} doped ZnO nanocrystals uniformly dispersed in nanofibers. Nanotechnology, 2011, 22, 415702.	1.3	25
96	Systematic study of the focal shift effect in planar plasmonic slit lenses. Nanotechnology, 2012, 23, 444002.	1.3	25
97	Towards low timing phase noise operation in fiber lasers mode locked by graphene oxide and carbon nanotubes at 15 Âμm. Optics Express, 2015, 23, 501.	1.7	25
98	Gibbs–Thomson Effect in Planar Nanowires: Orientation and Doping Modulated Growth. Nano Letters, 2016, 16, 4158-4165.	4.5	24
99	A Wide-Angle Broadband Converter: From Odd-Mode Spoof Surface Plasmon Polaritons to Spatial Waves. IEEE Transactions on Antennas and Propagation, 2019, 67, 7425-7432.	3.1	24
100	Band structure of Ge _{1â^'x} Sn _x alloy: a full-zone 30-band k · p model. New Journal of Physics, 2019, 21, 073037.	1.2	24
101	All-Fiber 3>tex<\$times\$>/tex<3 Interleaver Design With Flat-Top Passband. IEEE Photonics Technology Letters, 2004, 16, 168-170.	1.3	23
102	Reverse surface-polariton cherenkov radiation. Scientific Reports, 2016, 6, 30704.	1.6	23
103	Monolithic Semiconductor Lasers with Dynamically Tunable Linear-to-Circular Polarization. ACS Photonics, 2017, 4, 517-524.	3.2	23
104	Coherent emission from integrated Talbot-cavity quantum cascade lasers. Optics Express, 2017, 25, 3077.	1.7	23
105	Photonic Engineering Technology for the Development of Terahertz Quantum Cascade Lasers. Advanced Optical Materials, 2020, 8, 1900573.	3.6	23
106	Recent Progress in 2D Inorganic/Organic Charge Transfer Heterojunction Photodetectors. Advanced Functional Materials, 2022, 32, .	7.8	23
107	Electrically pumped semiconductor laser with low spatial coherence and directional emission. Applied Physics Letters, 2019, 115, .	1.5	22
108	Observation of Topological Edge States in Thermal Diffusion. Advanced Materials, 2022, 34, .	11.1	22

#	Article	IF	CITATIONS
109	Multi-beam multi-wavelength semiconductor lasers. Applied Physics Letters, 2009, 95, .	1.5	21
110	Transverse mode control in high-contrast grating VCSELs. Optics Express, 2014, 22, 20954.	1.7	21
111	Broadly tunable single-mode mid-infrared quantum cascade lasers. Journal of Optics (United) Tj ETQq1 1 0.78431	4 rgBT /O	verlock 10 Tf
112	Recent Developments of Terahertz Quantum Cascade Lasers. IEEE Journal of Selected Topics in Quantum Electronics, 2017, 23, 1-18.	1.9	21
113	Activation energy study of electron transport in high performance short wavelengths quantum cascade lasers. Optics Express, 2010, 18, 746.	1.7	20
114	Active Focal Length Control of Terahertz Slitted Plane Lenses by Magnetoplasmons. Plasmonics, 2012, 7, 191-199.	1.8	20
115	Low divergence single-mode surface-emitting concentric-circular-grating terahertz quantum cascade lasers. Optics Express, 2013, 21, 31872.	1.7	20
116	An all-optical plasmonic limiter based on a nonlinear slow light waveguide. Nanotechnology, 2012, 23, 444014.	1.3	19
117	Two-Dimensional Multimode Terahertz Random Lasing with Metal Pillars. ACS Photonics, 2018, 5, 2928-2935.	3.2	19
118	300  μJ, 3  W, few-cycle, 3  μm OPCPA based on periodically poled stoichiometric l Optics Letters, 2019, 44, 2791.	ithium tan 1.7	talate crysta
119	Ultracompact 2\$,imes,\$2 Photonic Crystal Waveguide Power Splitter Based on Self-Imaging Effect Realized by Asymmetric Interference. IEEE Photonics Technology Letters, 2011, 23, 1151-1153.	1.3	18
120	Magneto-plasmonics in graphene-dielectric sandwich. Optics Express, 2014, 22, 21727.	1.7	18
121	The reduction of surface plasmon losses in quasi-suspended graphene. Scientific Reports, 2015, 5, 9837.	1.6	18
122	Bright monolayer tungsten disulfide <i>via</i> exciton and trion chemical modulations. Nanoscale, 2018, 10, 6294-6299.	2.8	18
123	Tunable single-mode slot waveguide quantum cascade lasers. Applied Physics Letters, 2014, 104, .	1.5	17
124	Hybrid III–V/silicon laser with laterally coupled Bragg grating. Optics Express, 2015, 23, 8800.	1.7	17
125	Multistate Tuning of Third Harmonic Generation in Fanoâ€Resonant Hybrid Dielectric Metasurfaces. Advanced Functional Materials, 2021, 31, 2104627.	7.8	17
126	Switchable Unipolarâ€Barrier Van der Waals Heterostructures with Natural Anisotropy for Full Linear Polarimetry Detection. Advanced Materials, 2022, 34, .	11.1	17

#	Article	IF	CITATIONS
127	Near-field mapping of the edge mode of a topological valley slab waveguide at λ â€^ = 1.55 <i>μ </i> m. Applied Physics Letters, 2020, 116, .	1.5	16
128	Heterostrain-enabled dynamically tunable moiré superlattice in twisted bilayer graphene. Scientific Reports, 2021, 11, 21402.	1.6	16
129	Microscopic density matrix model for optical gain of terahertz quantum cascade lasers: Many-body, nonparabolicity, and resonant tunneling effects. Physical Review B, 2012, 86, .	1.1	15
130	50-W 2-μm Nanosecond All-Fiber-Based Thulium-Doped Fiber Amplifier. IEEE Journal of Selected Topics in Quantum Electronics, 2014, 20, 537-543.	1.9	15
131	Passively mode-locked III-V/silicon laser with continuous-wave optical injection. Optics Express, 2015, 23, 6392.	1.7	15
132	Wafer-Scale Dies-Transfer Bonding Technology for Hybrid III/V-on-Silicon Photonic Integrated Circuit Application. IEEE Journal of Selected Topics in Quantum Electronics, 2016, 22, 443-454.	1.9	15
133	Enhanced light-matter interaction in atomically thin MoS_2 coupled with 1D photonic crystal nanocavity. Optics Express, 2017, 25, 14691.	1.7	15
134	Flexible single-mode delivery of a high-power 2  μm pulsed laser using an antiresonant hollow-core fiber. Optics Letters, 2018, 43, 2732.	1.7	15
135	Photon-generated carrier transfer process from graphene to quantum dots: optical evidences and ultrafast photonics applications. Npj 2D Materials and Applications, 2020, 4, .	3.9	15
136	Flatâ€Top Pumped Multiâ€Millijoule Midâ€Infrared Parametric Chirpedâ€Pulse Amplifier at 10ÂkHz Repetition Rate. Laser and Photonics Reviews, 2021, 15, 2000292.	4.4	15
137	Emission properties of electrically pumped triangular shaped microlasers. Optics Express, 2010, 18, 16437.	1.7	13
138	Analysis of dielectric loaded surface plasmon waveguide structures: Transfer matrix method for plasmonic devices. Journal of Applied Physics, 2012, 111, 073108.	1.1	13
139	Importance of the microscopic effects on the linewidth enhancement factor of quantum cascade lasers. Optics Express, 2013, 21, 27804.	1.7	13
140	Plasmon excitation on flat graphene by s-polarized beams using four-wave mixing. Optics Express, 2015, 23, 7809.	1.7	13
141	65-fs Pulses at 2 \$mu ext{m}\$ in a Compact Tm-Doped All-Fiber Laser by Dispersion and Nonliearity Management. IEEE Photonics Technology Letters, 2018, 30, 303-306.	1.3	13
142	NOx Measurements in Vehicle Exhaust Using Advanced Deep ELM Networks. IEEE Transactions on Instrumentation and Measurement, 2021, 70, 1-10.	2.4	13
143	Tailorable infrared emission of microelectromechanical system-based thermal emitters with NiO films for gas sensing. Optics Express, 2021, 29, 19084.	1.7	13
144	Spatial structure of lasing modes in wave-chaotic semiconductor microcavities. New Journal of Physics, 2020, 22, 083002.	1.2	13

#	:	Article	IF	CITATIONS
14	45	High-energy mid-infrared intrapulse difference-frequency generation with 53% conversion efficiency driven at 3 µm. Optics Express, 2019, 27, 37706.	1.7	13
14	46	Long-wavelength-infrared laser filamentation in solids in the near-single-cycle regime. Optics Letters, 2020, 45, 2175.	1.7	13
14	47	Design of three-well indirect pumping terahertz quantum cascade lasers for high optical gain based on nonequilibrium Green's function analysis. Applied Physics Letters, 2012, 100, .	1.5	12
14	48	Synthetic jet generation by high-frequency cavitation. Journal of Fluid Mechanics, 2017, 823, .	1.4	12
14	49	W-type normal dispersion thulium-doped fiber-based high-energy all-fiber femtosecond laser at 1.7  µm. Optics Letters, 2021, 46, 3637.	1.7	12
1	50	Plasmon-induced thermal tuning of few-exciton strong coupling in 2D atomic crystals. Optica, 2021, 8, 1416.	4.8	12
1	51	20 W, 2 mJ, sub-ps, 258â€nm all-solid-state deep-ultraviolet laser with up to 3 GW peak power. Optics Express, 2020, 28, 18360.	1.7	12
1	52	Nanoâ€Optical Engineering of Anisotropic Phonon Resonances in a Hyperbolic αâ€MoO ₃ Metamaterial. Advanced Optical Materials, 2022, 10, .	3.6	12
1	53	Flat-passband 3 /spl times/ 3 interleaving filter designed with optical directional couplers in lattice structure. Journal of Lightwave Technology, 2005, 23, 4349-4362.	2.7	11
1	54	The Influence of Imperfections and Absorption on the Performance of a GaAs/AlO \$_{m x}\$ High-Contrast Grating for Monolithic Integration With 980 nm GaAs-Based VCSELs. Journal of Lightwave Technology, 2013, 31, 3853-3858.	2.7	11
1	55	Planar integrated metasurfaces for highly-collimated terahertz quantum cascade lasers. Scientific Reports, 2014, 4, 7083.	1.6	11
1	56	Quantitative Analysis of Gas Phase IR Spectra Based on Extreme Learning Machine Regression Model. Sensors, 2019, 19, 5535.	2.1	11
1	57	Surface group-modified MXene nano-flake doping of monolayer tungsten disulfides. Nanoscale Advances, 2019, 1, 4783-4789.	2.2	11
1	58	β-In ₂ S ₃ Nanoplates for Ultrafast Photonics. ACS Applied Nano Materials, 2022, 5, 3229-3236.	2.4	11
1	59	Fundamental frequency noise and linewidth broadening caused by intrinsic temperature fluctuations in quantum cascade lasers. Physical Review B, 2011, 84, .	1.1	10
10	60	The Transition from Quantum Field Theory to One-Particle Quantum Mechanics and a Proposed Interpretation of Aharonov–Bohm Effect. Foundations of Physics, 2018, 48, 837-852.	0.6	10
10	61	Laser-mode bifurcations induced by <mml:math xmlns:mml="http://www.w3.org/1998/Math/MathML"><mml:mi mathvariant="script">PT -breaking exceptional points. Physical Review A, 2019, 99</mml:mi </mml:math 	1.0	10
10	62	Directing Cherenkov photons with spatial nonlocality. Nanophotonics, 2020, 9, 3435-3442.	2.9	10

#	Article	IF	CITATIONS
163	Track-and-Tune Light Field Image Sensor. IEEE Sensors Journal, 2014, 14, 4372-4384.	2.4	9
164	155 Âμm high speed low chirp electroabsorption modulated laser arrays based on SAG scheme. Optics Express, 2014, 22, 31286.	1.7	9
165	Three-region characteristic temperature in p-doped quantum dot lasers. Applied Physics Letters, 2014, 104, 041102.	1.5	9
166	Sizeâ€induced Switching of Nanowire Growth Direction: a New Approach Toward Kinked Nanostructures. Advanced Functional Materials, 2016, 26, 3687-3695.	7.8	9
167	High-efficiency ultrafast Tm-doped fiber amplifier based on resonant pumping. Optics Letters, 2018, 43, 1431.	1.7	9
168	Multimode lasing in wave-chaotic semiconductor microlasers. Physical Review A, 2019, 100, .	1.0	9
169	Design of spectrum equalization filter for SLED light source. Optics Communications, 2004, 229, 223-231.	1.0	8
170	Graphene Enhanced Surface Plasmon Resonance Fiber-Optic Biosensor. , 2016, , .		8
171	Compact pulsed thulium-doped fiber laser for topographical patterning of hydrogels. Opto-Electronic Advances, 2020, 3, 190039-190039.	6.4	8
172	Single-mode lasing based on <mml:math xmlns:mml="http://www.w3.org/1998/Math/MathML"><mml:mi mathvariant="script">PT</mml:mi </mml:math> -breaking of two-dimensional photonic higher-order topological insulator. Physical Review B, 2021, 104, .	1.1	8
173	Sensitive control of broad-area semiconductor lasers by cavity shape. APL Photonics, 2022, 7, .	3.0	8
174	Design of 100/300 GHz optical interleaver with IIR architectures. Optics Express, 2005, 13, 2643.	1.7	7
175	A single-walled carbon nanotube wall paper as an absorber for simultaneously achieving passively mode-locked and Q-switched Yb-doped fiber lasers. , 2013, , .		7
176	Coherent Pulse Progression of Mid-Infrared Quantum-Cascade Lasers Under Group-Velocity Dispersion and Self-Phase Modulation. IEEE Journal of Quantum Electronics, 2016, 52, 1-6.	1.0	7
177	Optimization of TM modes for amorphous slab lasers. Optics Express, 2016, 24, 4890.	1.7	7
178	Probing electron–atom collision dynamics in gas plasma by high-order harmonic spectroscopy. Optics Letters, 2018, 43, 1970.	1.7	7
179	Tunability of the Freeâ€Spectral Range by Microwave Injection into a Midâ€Infrared Quantum Cascade Laser. Laser and Photonics Reviews, 2020, 14, 1900389.	4.4	7
180	Germaniumâ€onâ€Carborundum Surface Phononâ€Polariton Infrared Metamaterial. Advanced Optical Materials, 2021, 9, 2001652.	3.6	7

#	Article	IF	CITATIONS
181	Photonic crystal MEMS emitter for chemical gas sensing. , 2021, , .		7
182	Directional single-mode emission from coupled whispering gallery resonators realized by using ZnS microbelts. Optics Letters, 2013, 38, 1527.	1.7	6
183	Self-compression of mJ pulses to 10  fs in a hollow-core waveguide: effects of higher-order dispersion. Journal of the Optical Society of America B: Optical Physics, 2022, 39, A1.	0.9	6
184	Surface-emitting THz sources based on difference-frequency generation in mid-infrared quantum cascade lasers. Proceedings of SPIE, 2010, , .	0.8	5
185	Effects of resonant tunneling and dynamics of coherent interaction on intrinsic linewidth of quantum cascade lasers. Optics Express, 2012, 20, 17145.	1.7	5
186	Optical Properties of GaAs/AlO <formula formulatype="inline"><tex Notation="TeX">\$_{x}\$</tex </formula> and Si/SiO <formula formulatype="inline"><tex notation="TeX">\$_{x}\$</tex> High Contrast Gratings Designed for 980-nm VCSELs. IEEE Nanotechnology Magazine, 2014, 13, 418-424.</formula 	1.1	5
187	Broadly continuously tunable slot waveguide quantum cascade lasers based on a continuum-to-continuum active region design. Applied Physics Letters, 2015, 107, 111110.	1.5	5
188	Optimization of Hybrid Silicon Lasers for High-Speed Direct Modulation. IEEE Photonics Journal, 2015, 7, 1-13.	1.0	5
189	Ground-state lasing in high-power InAs/GaAs quantum dots-in-a-well laser using active multimode interference structure. Optics Letters, 2015, 40, 69.	1.7	5
190	Optimization of spectral distortion in a ytterbium-doped mode-locked fiber laser system. Photonics Research, 2015, 3, 129.	3.4	5
191	Surface roughness measurement by depolarization method. Applied Optics, 2015, 54, 5686.	2.1	5
192	High Energy Ultrafast Laser at 2 μm Using Dispersion Engineered Thulium-Doped Fiber. IEEE Photonics Journal, 2019, 11, 1-12.	1.0	5
193	Scattering by lossy anisotropic scatterers: A modal approach. Journal of Applied Physics, 2021, 129, .	1.1	5
194	Long wavelength (λ > 13 μm) quantum cascade laser based on diagonal transition and three-phonon-resonance design. Applied Physics Letters, 2021, 119, .	1.5	5
195	Producing Microscale Ge Textures via Titanium Nitride―and Nickelâ€Assisted Chemical Etching with CMOSâ€Compatibility. Advanced Materials Interfaces, 2021, 8, 2100937.	1.9	5
196	Reply to: Detectivities of WS2/HfS2 heterojunctions. Nature Nanotechnology, 2022, 17, 220-221.	15.6	5
197	Widely tunable single-mode slot waveguide quantum cascade laser array. Optics Express, 2022, 30, 629.	1.7	5
198	A stable dual-wavelength channel-selectable erbium-doped fiber ring laser using channel wavelength generator. Optics Communications, 2003, 225, 89-94.	1.0	4

#	Article	IF	CITATIONS
199	Equalization of Gaussian-like spectra with optical lattice filters. Journal of the Optical Society of America B: Optical Physics, 2005, 22, 1498.	0.9	4
200	Design of linear-phase two-port optical interleavers using lattice architectures. Optics Letters, 2006, 31, 2411.	1.7	4
201	Voigt Airy surface magneto plasmons. Optics Express, 2012, 20, 21187.	1.7	4
202	Microjoule Sub-Two-Cycle Mid-Infrared Intrapulse-DFG Driven by 3-\$mu\$ m OPCPA. IEEE Photonics Technology Letters, 2019, 31, 1741-1744.	1.3	4
203	Coupling of sub-Terawatt Laser into Hollow Core Waveguide for High Harmonic Generation above 200 eV. IEEE Photonics Technology Letters, 2020, , 1-1.	1.3	4
204	Band Structure of Strained \$mathrm{Ge}_{1-x}~mathrm{Sn}_{x}\$ Alloy: A Full-Zone 30-Band \${k}cdot{p}\$ Model. IEEE Journal of Quantum Electronics, 2020, 56, 1-8.	1.0	4
205	Polarization-robust mid-infrared carpet cloak with minimized lateral shift. Photonics Research, 2021, 9, 944.	3.4	4
206	A conformal transformation approach to wide-angle illusion device and absorber. Nanophotonics, 2020, 9, 3243-3249.	2.9	4
207	Theoretical design of mid-infrared interband cascade lasers in SiGeSn system. New Journal of Physics, 2020, 22, 083061.	1.2	4
208	Relative Intensity Noise of Silicon Hybrid Laser. IEEE Journal of Quantum Electronics, 2014, 50, 466-473.	1.0	3
209	High-contrast grating reflectors for 980 nm vertical-cavity surface-emitting lasers. , 2015, , .		3
210	Terahertz emission from localized modes in one-dimensional disordered systems [Invited]. Photonics Research, 2018, 6, 117.	3.4	3
211	A heavily doped germanium pyramid array for tunable optical antireflection in the broadband mid-infrared range. Journal of Materials Chemistry C, 2022, 10, 5797-5804.	2.7	3
212	Broad-band RF Photonic Phase Modulator Based on a Novel Nonlinear Optical Loop Mirror. , 2006, , .		2
213	Cost-effective optical modulation depth enhancement and optical carrier recovery in millimeter-wave fiber-wireless links using an all-fiber optical interleaver. , 2006, , .		2
214	An efficient all-fiber interleaving filter using fiber Gires-Tournois etalons on a Michelson interferometer. , 2006, , .		2
215	Optical Fiber Polarization Interferometer for Performance Improvement in Radio-Over-Fiber Systems. IEEE Photonics Technology Letters, 2007, 19, 1236-1238.	1.3	2
216	Tunable Terahertz plasmonic lens with external magnetic field. , 2010, , .		2

#	Article	IF	CITATIONS
217	All-fiber all-normal-dispersion passively mode-locked Yb-doped ring laser based on graphene oxide. , 2012, , .		2
218	Investigation of Tunable Single-Mode Quantum Cascade Lasers Via Surface-Acoustic-Wave Modulation. IEEE Journal of Quantum Electronics, 2013, 49, 1053-1061.	1.0	2
219	Fiber profilometer for measurement of hard-to-access areas. , 2013, , .		2
220	Magnetopolariton in bilayer graphene: A tunable ultrastrong light-matter coupling. Physical Review B, 2014, 89, .	1.1	2
221	High-resolution fiber profilometer for hard-to-access areas. Applied Optics, 2015, 54, 7205.	2.1	2
222	Integrated terahertz optoelectronics. , 2016, , .		2
223	High-energy single-cycle pulse generation in a parametric amplifier with the optimized angular dispersion. Applied Physics B: Lasers and Optics, 2019, 125, 1.	1.1	2
224	Terahertz Quantum Cascade Lasers with Integrated Plasmonic Collimators. , 2010, , .		2
225	Terahertz Graphene Modulator Integrated with Quantum Cascade Laser Achieving 100% Modulation Depth. , 2016, , .		2
226	Equalization of Gaussian-Like Spectra via Optical Lattice Filters With Symmetric-Feedback Structure. Journal of Lightwave Technology, 2006, 24, 5103-5110.	2.7	1
227	Linear-phase fiber lattice equalizer for Gaussian-like spectra. Optical Engineering, 2006, 45, 080507.	0.5	1
228	Gaussian-like spectra equalization with linear-phase lattice filters. Journal of the Optical Society of America B: Optical Physics, 2007, 24, 615.	0.9	1
229	Radio-over-Fiber Transmission of 1.25-Gigabit Ethernet Signal on 60-GHz Band Subcarrier with Performance Improvement and Wavelength Reuse. , 2007, , .		1
230	Tunable subwavelength terahertz plasmonic stub waveguide filters. , 2013, , .		1
231	Graphene-based tunable Bragg reflector with a broad bandwidth. , 2014, , .		1
232	Nano-imaging collagen by atomic force, near-field and nonlinear microscope. Proceedings of SPIE, 2015, , .	0.8	1
233	Ultrastrong light-matter coupling of cyclotron transition in monolayer <mml:math xmlns:mml="http://www.w3.org/1998/Math/MathML"><mml:mrow><mml:mi>Mo</mml:mi><mml:msub><mml:m mathvariant="normal">S<mml:mn>2</mml:mn></mml:m </mml:msub></mml:mrow>. Physical Review B. 2016. 93</mml:math 	¹ⁱ 1.1	1
234	Superradiant phase transition with graphene embedded in one dimensional optical cavity. Superlattices and Microstructures, 2018, 113, 401-408.	1.4	1

#	Article	IF	CITATIONS
235	1975 nm Linearly-Polarized MOFA CPA System Based on CFBG Stretcher and 1+3-Pass CVBG Compressor Configuration. , 2019, , .		1
236	Mid-Infrared Grayscale Metasurface Holograms. Applied Sciences (Switzerland), 2020, 10, 552.	1.3	1
237	High-energy Pulse Generation at 1.76 μm from All-fiber Laser Configuration using Normal Dispersion Thulium-doped Fiber. , 2020, , .		1
238	Visible Range Plasmons in Topological Insulators. , 2016, , .		1
239	Tm/Ho co-doped mode-locked fiber laser based on graphene transferred on side-polished fiber. , 2015, , .		1
240	Amorphous Random Lasing at Terahertz Frequency. , 2016, , .		1
241	Guiding and routing surface plasmons with transformation-invariant metamaterials. Journal of Optics (United Kingdom), 2022, 24, 015003.	1.0	1
242	Multistate Tuning of Third Harmonic Generation in Fanoâ€Resonant Hybrid Dielectric Metasurfaces (Adv. Funct. Mater. 48/2021). Advanced Functional Materials, 2021, 31, .	7.8	1
243	SLED equalization using all-fiber unbalanced Mach-Zehnder interferometer. , 0, , .		Ο
244	Channel-wavelength-selectable multiwavelength ring laser using a cascaded fiber MZ interferometer and a EDFA. , 2003, , .		0
245	Low divergence semiconductor lasers by plasmonic collimation. , 2008, , .		Ο
246	High performance room temperature quantum cascade lasers based on three-phonon-resonance depopulation. , 2008, , .		0
247	Wavefront engineering of semiconductor lasers using plasmonics. , 2010, , .		Ο
248	GaAs/Al <inf>0.15</inf> Ga <inf>0.85</inf> As terahertz quantum cascade lasers with double-phonon resonant depopulation operating up to 172 K. , 2011, , .		0
249	Single-mode narrow beam divergence surface-emitting concentric-circular-grating terahertz quantum cascade lasers. , 2012, , .		Ο
250	Effects of resonant tunneling on intrinsic linewidth of quantum cascade lasers. , 2012, , .		0
251	Linewidth broadening caused by intrinsic temperature fluctuations in quantum cascade lasers. , 2012, , \cdot		0
252	Mid-infrared Bessel beams generation by subwavelength structure on quantum cascade laser. , 2012, , .		0

#	Article	IF	CITATIONS
253	Microscopic analysis on optical gain of terahertz quantum cascade lasers. , 2012, , .		Ο
254	Micro-cavity lasers with directional emission. , 2012, , .		0
255	Quantum cascade lasers of λ ≈ 14µm based on three-phonon-resonance design. , 2012, , .		Ο
256	A one-way terahertz plasmonic waveguide based on surface magneto plasmons in a metal-dielectric-semiconductor structure. , 2013, , .		0
257	Comparison of timing noise properties of carbon nanotubes, graphene and graphene oxide as saturable absorbers for a mode-locked Er-doped fiber laser. , 2013, , .		Ο
258	OPTICAL GAIN AND ENERGY BAND STRUCTURE OF PHOTONIC CRYSTAL VCSELs WITH HIGH-INDEX-CONTRAST SUBWAVELENGTH GRATINGS. Journal of Molecular and Engineering Materials, 2014, 02, 1440014.	0.9	0
259	Mid-infrared Disordered Photonic Crystal Lasers. , 2014, , .		Ο
260	1 micrometer wavelength pulse fiber laser assisted black marking on the surface of aluminum oxide. , 2015, , .		0
261	Surface plasmon polariton generation using acousto-optic effect in fiber. , 2015, , .		Ο
262	Multiwavelength thulium-doped fiber laser based on four-wave mixing in highly germania-doped fiber. , 2015, , .		0
263	Passively mode-locked III-V/silicon lasers with low time jitter using CW optical injection. , 2015, , .		Ο
264	Widely tunable multi-wavelength Tm-doped mode-locked fiber laser. , 2016, , .		0
265	High-efficiency pulsed Tm-doped fiber amplifier. , 2017, , .		0
266	2-micron Pulse compression using gas-filled negative curvature hollow-core fiber. , 2017, , .		0
267	Three-fold efficiency improvement via temporal and spatial pulse shaping in 3 ν m OPCPA. , 2017, , .		0
268	Ultra confined polaritons in atomically layered dielectrics. , 2017, , .		0
269	Terahertz Emission in One-Dimensional Disordered Systems. , 2017, , .		0
270	Random Lasers in the Mid-infrared and Terahertz regimes. , 2017, , .		0

16

#	Article	IF	CITATIONS
271	Tunable Mode-Locked Fiber Laser in 1750–1870nm by Bending Normal Dispersion Thulium-Doped Fiber as a Distribution Filter. , 2019, , .		0
272	A generalized analytical model of gain bandwidth for design of optical parametric amplifiers. Optics Communications, 2019, 449, 1-7.	1.0	0
273	Spatio-Temporal Dynamics of Microlasers with Chaotic Ray Dynamics. , 2019, , .		0
274	Highly parallel ultra-fast random number generation from a stable-cavity broad-area semiconductor laser. , 2021, , .		0
275	All-fiber High-energy 174 fs Laser at 1.78 μ m using parabolic W-type Normal Dispersion Thulium-doped Fiber. , 2021, , .		0
276	Gain competition in multicolor Quantum Cascade Lasers. , 2010, , .		0
277	Highly unidirectional whispering gallery mode lasers. , 2011, , .		0
278	Mid-infrared Raman sources with highly GeO2-doped silica optical fibers. , 2015, , .		0
279	Broadband quantum cascade laser at wavelength λ~10 μm based on continuum-to-continuum design. , 2015, , .		Ο
280	High performance index-coupled distributed feedback InAs/GaAs quantum dots-in-a-well lasers with laterally corrugated waveguides. , 2016, , .		0
281	Microjoule sub-three-cycle long-wavelength intrapulse difference frequency generation driven at 3 μm. , 2019, , .		Ο
282	Far-field controllable excitation of phonon polariton via nanostructure engineering. Optics Express, 2020, 28, 39156.	1.7	0
283	20 W, 2.0 mJ, sub-ps deep-ultraviolet laser at 258 nm. , 2020, , .		Ο
284	Planar Resonators Supporting Extremely Confined Phonon-Polariton Modes. , 2020, , .		0
285	Spatio-temporal dynamics of highly multimode semiconductor lasers. , 2020, , .		Ο
286	All-fiber Short-wavelength Mode-locked Fiber Laser and Amplifier Using Normal Dispersion Thulium-doped Fiber. , 2020, , .		0
287	Broad-area semiconductor laser for ultrafast parallel random number generation. , 2021, , .		0
288	Parallel Generation of Random Numbers Using a Broad-area Stable-cavity Semiconductor Laser. , 2021, ,		0

#	Article	IF	CITATIONS
289	Ultrafast parallel random number generation with a chip-scale semiconductor laser. , 2021, , .		Ο
290	Strain engineering for pseudo-magnetic fields in graphene. , 2022, , .		0
291	Study of carrier dynamics in strained graphene with giant pseudo-magnetic fields. , 2022, , .		Ο
292	Filament Based Self-Compression of 100 GW Ultrashort Pulses in Ar Filled Capillary. , 2022, , .		0